
ON THE LOSS OF CONTEXT-AWARENESS IN GENERAL INSTRUCTION FINE-TUNING

Yihan Wang*

UCLA

wangyihan617@gmail.com

Andrew Bai*

UCLA

andrewbai@ucla.edu

Nanyun Peng

UCLA

violetpeng@cs.ucla.edu

Cho-Jui Hsieh

UCLA

chohsieh@cs.ucla.edu

ABSTRACT

Pre-trained Large Language Models (LLMs) require post-training methods such as supervised fine-tuning (SFT) on instruction-response pairs to enable instruction following. However, this process can potentially harm existing capabilities learned during pre-training. In this paper, we investigate the loss of context awareness after SFT, where context awareness is defined as the ability to extract and understand information from user-provided context and respond accordingly. We are the first to identify and show that the loss of context awareness, as reflected by the performance drop in the Needle-in-a-Haystack test, occurs in instruction fine-tuned LLMs when the chat template is applied to input prompts. We identify that the performance decline is partially caused by an attention bias toward different roles learned during conversational instruction fine-tuning. We validate our hypothesis by visualizing changes in attention allocation after the chat template is applied and manually steering the attention heads. Based on these observations, we propose a metric to select context-dependent examples from general instruction fine-tuning datasets. We then apply conditional instruction fine-tuning with a context-dependency indicator, enabling the model to learn context awareness from these selected examples. Empirical experiments on four context-dependent downstream tasks and three pre-trained LLMs of different sizes show that our method effectively mitigates the loss of context awareness without compromising general instruction-following capabilities. Given our findings, we strongly advocate for careful benchmarking of context awareness after instruction fine-tuning.

1 Introduction

Large language models (LLMs) pretrained on large-scale datasets acquire diverse language skills during pretraining. To enhance these models' ability to follow general instructions, further fine-tuning is typically required. This includes supervised instruction fine-tuning (SFT) (Wei et al., 2021; Ouyang et al., 2022) and reinforcement learning from human feedback (RLHF) (Christiano et al., 2017). However, several studies have demonstrated additional fine-tuning can potentially harm existing capabilities learned during pretraining (Lin et al., 2024; Bai et al., 2022; Fu et al., 2024).

Although some studies suggest that performance degradation can be mitigated or even eliminated through improved instruction fine-tuning methods (Longpre et al., 2023; Bai et al., 2022; Glaese et al., 2022), in this paper, we demonstrate that instruction fine-tuning specifically leads to the worsening of a model's context awareness. Context awareness is defined as a model's ability to accurately retrieve, process, and interpret specific information from user-provided context. Context awareness is highly relevant to the *intrinsic hallucinations* of LLMs (Huang et al., 2023) and crucial to the truthfulness of LLM-based chat models (Ouyang et al., 2022). It is also important for many real-world use cases, including retrieval augmented generalization (Khandelwal et al., 2020; Izacard et al., 2023; Xu et al., 2023b),

*Equal contribution

Code is available at https://github.com/YihanWang617/context_awareness.

in-context learning (Agarwal et al., 2024), and contextual question-answering (Rajpurkar et al., 2016; Choi et al., 2018; Dua et al., 2019).

We demonstrate the loss of context awareness through evaluations of several popular, open-source LLMs using the Needle-in-a-Haystack (NIH) test (Kamradt, 2023), which requires a model to retrieve a given text “needle” from a long paragraph of irrelevant text. Performance on NIH tests deteriorates consistently after instruction fine-tuning across pretrained LLMs, regardless of their context window sizes, chat templates, architectures, or model sizes. Our analysis reveals that the decline in NIH performance is directly correlated with the application of chat templates during the instruction fine-tuning and inference phases. When these chat templates are not applied to instruction fine-tuned models, NIH performance not only recovers but in some instances surpasses that of their pretrained, non-fine-tuned counterparts.

These observations suggest that the deterioration in NIH performance does not indicate a catastrophic loss of context-retrieval capabilities during instruction fine-tuning. Instead, the chat template appears to mask these underlying abilities by introducing systematic biases into the models’ behavior. Through analysis, we observe differences in attention allocation patterns in input tokens when comparing instruction fine-tuned models with and without applying chat templates. Specifically, we examine how the attention allocation shifts when tokens are marked as “user tokens” by the chat template. As illustrated in Figure 3, the application of chat templates leads to a redistribution of attention values: attention scores decrease for user input tokens while increasing for assistant tokens. We validate the relationship between attention score reallocation and context awareness through targeted intervention experiments. By manually increasing attention values assigned to user tokens, we partially restored the NIH performance. This confirms a direct connection between attention allocation and context processing capabilities.

These findings motivate us to develop a fine-tuning strategy that mitigates attention bias acquired during instruction fine-tuning. Our approach stems from the intuition that the bias is learned from certain patterns in the training dataset. We develop a quantitative metric to assess the context-dependency of conversational instruction and response pairs based on attention allocation patterns. With this analysis, we discover that context-dependent examples are notably sparse in commonly used open-source instruction fine-tuning datasets. To address the limitation, we add an indicator token to the identified context-dependent instructions. After fine-tuning the model with this enhanced dataset, it learns to allocate increased attention to user tokens when the indicator is present.

Our method is evaluated through experiments across three pretrained language models and four context-dependent tasks. Empirical results demonstrate that models fine-tuned using our method consistently achieve superior performance on context-dependent tasks compared to standard fine-tuning while maintaining similar performance on general tasks.

Our contributions are summarized as follows:

- We identify that the context awareness of LLMs deteriorates after supervised instruction fine-tuning with chat templates applied, as measured by the performance drop on the NIH task.
- We pinpoint that the worsened context awareness is associated with attention allocation bias on tokens marked as from different roles.
- We propose a quantitative metric to identify context-dependent instruction-response pairs from general instruction fine-tuning datasets.
- We propose a fine-tuning strategy to insert a context-dependency indicator into identified instructions during instruction fine-tuning and mitigate the loss of context awareness by appending the indicator to instructions during inference.

2 Loss of context awareness after Instruction Finetuning

2.1 Evaluating Context Awareness Through Needle-in-a-Haystack (NIH) Testing

In this section, we demonstrate the loss of context awareness after instruction fine-tuning with the needle-in-a-haystack (NIH) test.

Dataset. The NIH test evaluates the performance of language models in extracting a given sentence (the needle) from irrelevant context. The needle can be inserted at different locations in contexts of varying lengths. We report the recall error:

$$\text{err} = \frac{1}{|K|} \sum_{w \in K} \mathbb{1}(w \in \text{output})$$

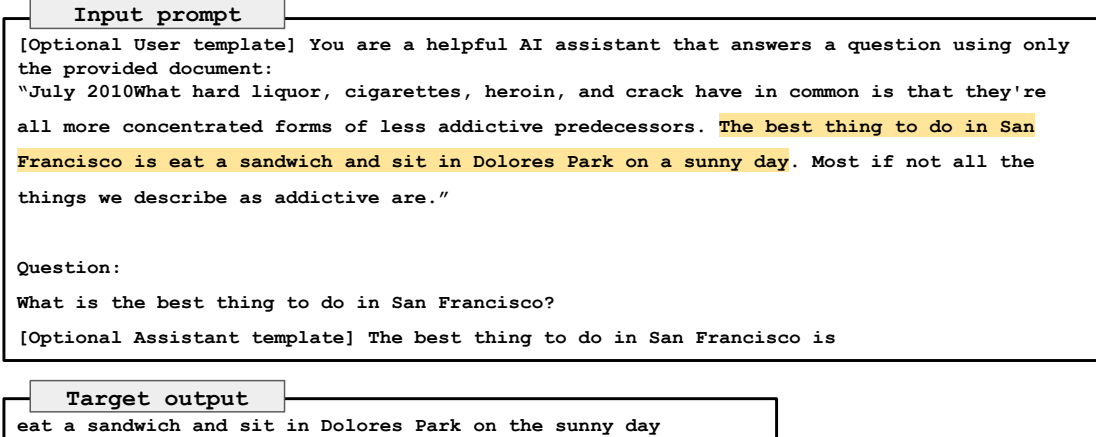


Figure 1: An example of the Needle-in-a-haystack (NIH) test used in our work. [Optional User template] and [Optional Assistant template] are user and assistant role indicators used in instruction finetuned models. The inserted needle is highlighted in yellow.

where K is the set of keywords in the targeted output and $output$ is the output of the LLM. We average the recall error across 400 NIH tests with different insertion locations and context lengths within the model’s context window. An example of the NIH prompt in our experiments is shown in Figure 1. When the chat template is applied to the prompt, the whole input prompt is partitioned into the user instruction input and model response, indicated by special role markers in the chat template (e.g., $<|\text{user}|>$ and $<|\text{assistant}|>$). More details about the NIH tests can be found in Appendix A.2.

Models. We evaluate NIH on eight open-source language models from five model families with their corresponding chat templates. For each model, we compare the performance of the pretrained version (not instruction fine-tuned) and the official instruction-finetuned version released by the model provider. Here, we do not consider stronger closed-source models as their pretrained versions are unavailable. The context window lengths of these models range from $4K$ to $32K$.

NIH performance drops after instruction finetuning on most models. We report the evaluation results on NIH in Figure 2. Given the improved instruction-following through instruction finetuning, we would expect that performance would increase on general tasks. However, when comparing the pretrained model (green bar) with the instruction-finetuned model (red bar), the NIH error *increases* for most models after instruction fine-tuning.

The performance drop is associated with chat templates. To determine whether the performance difference mainly comes from a different input format or fine-tuned model weights, we remove the chat templates (i.e., the role indicators in instruction-tuned models) and visualize the NIH errors with blue bars in Figure 3. The NIH error without applying chat templates (blue bar) is significantly lower than with templates (red bar). These results indicate that context retrieval capabilities are not eliminated by instruction fine-tuning, but are instead impacted by biases associated with the presence of chat templates.

The aforementioned phenomenon is consistent across models with different context window lengths, model families, chat templates, and model sizes.

2.2 Attention Allocation Bias Across Different Roles

Based on our observations, performance on NIH drops significantly when the chat template is applied. We hypothesize that the performance deterioration stems from the bias in instruction data and the bias is embedded in different roles marked by the chat template. When the model generates a response, it balances information from the input context and internal knowledge stored within its weights. It pays attention to user tokens to maintain consistency with the user-provided context while attending to previously generated assistant response tokens to maintain consistency with its output. If the model learns during fine-tuning that its internal knowledge is more important for generating high-quality responses, it may develop a bias that causes it to weigh user tokens less heavily. To verify our hypothesis, we visualize and compare the attention allocation between user and assistant tokens, both with and without chat templates.

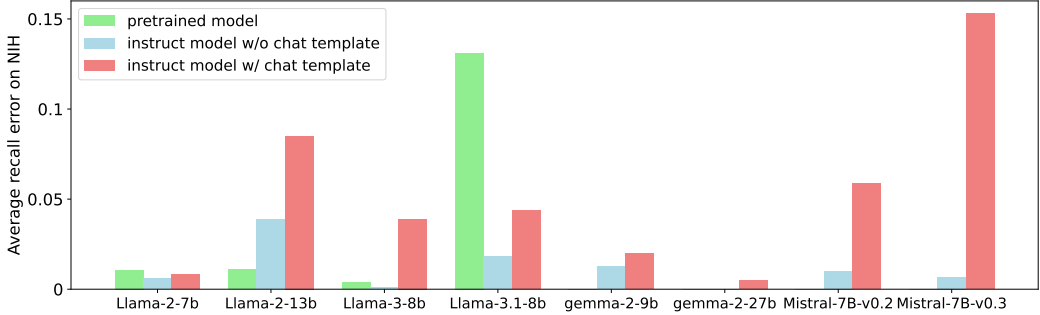


Figure 2: Average recall error ($1 - \text{recall}$) on NIH for different model series. We report the performance of official instruction-tuned models (both with and without chat templates) and their corresponding pretrained models from five model families, with sizes ranging from 7B to 27B. Note: Recall errors for some models are too small to be visible in the figure. Detailed numerical values can be found in Appendix B.1

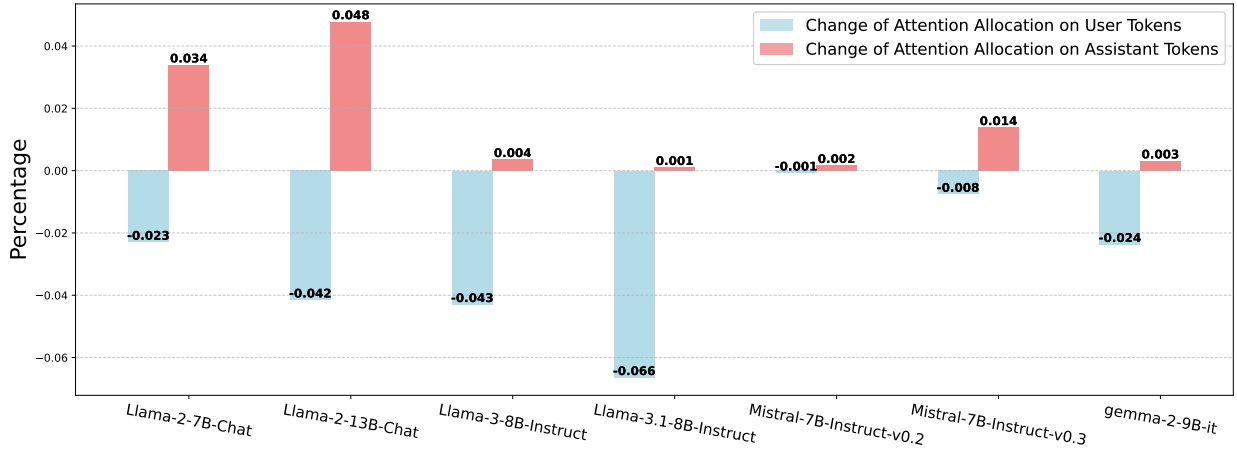


Figure 3: We visualize the changes in attention allocation between user tokens and assistant tokens after applying chat templates. The attention allocation is calculated when the model generates the first answer token in its response. For cases where a chat template is applied, we normalize the attention values on user tokens, assistant tokens, and the BOS token so that their combined attention scores sum to 1. The attention weights are averaged across 400 tests with context lengths ranging from 200 to 4,000 and needle depths from 0% to 100%. Detailed absolute attention scores for each component can be found in Appendix B.2.

Experimental settings. We prepare two inputs for each NIH test case: one with the chat template and one without. The prompt formats follow the input prompt shown in Figure 1. We collect attention weights from each layer, focusing on the last token (which generates the next answer token) and its attention to all input tokens. We separately sum the attention weights for user and assistant tokens. When calculating the attention weight allocation with chat templates, we exclude the attention weights on chat template tokens and renormalize the attention weights across the user, assistant, and BOS tokens. We report the attention allocation from an arbitrary middle layer (e.g., Layer 15) on a representative context retrieval head that allocates the highest attention to user tokens without chat templates. Further discussion on head and layer selection can be found in the Appendix B.3.

Less attention on user tokens with chat templates. We visualize the changes in attention allocation, both with and without chat templates in Figure 3. When chat templates are applied to mark tokens as from different roles, attention allocated to user tokens decreases while attention to assistant tokens increases for all models. This indicates that the models learn to assign lower attention to user tokens compared to the baseline level (where the chat template is not applied). In our experiments, we collect attention allocation data for context lengths less than 4,000. Although several models (e.g. Llama-3 and Gemma-2) achieve perfect NIH accuracy under 4,000 context length, the decrease in user attention remains noticeable.

2.3 Attention Steering to Compensate for Attention Bias

In the previous section, we observed a trend of decreased attention allocated to user tokens when chat templates were applied to instructional models, associated with a performance decline on the NIH task. A natural approach to mitigate this performance loss and further verify our hypothesis is to manually steer attention toward user tokens to compensate for the attention bias.

Post-hoc attention steering of user tokens. To compensate for the attention bias observed in instruction models, we manually steer the attention on user tokens.

Specifically, we modify the self-attention weights in each transformer layer:

$$\hat{\text{Att}}(\mathbf{x}, \mathbf{y}) = \begin{cases} \frac{1}{Z} \cdot \text{Att}(\mathbf{x}, \mathbf{y}) & \text{if } \mathbf{y} \in U \\ \frac{1}{Z} \cdot \alpha \text{Att}(\mathbf{x}, \mathbf{y}) & \text{otherwise,} \end{cases} \quad (1)$$

where \mathbf{x} and \mathbf{y} are two tokens in the input sequence, $0 < \alpha < 1$, U is the subset of all user tokens, and Z is the normalization constant that renormalizes the altered attention scores across all tokens. $\text{Att}(\mathbf{x}, \mathbf{y})$ is the original attention weight from token \mathbf{x} to token \mathbf{y} .

We adopt the same attention steering implementation as Zhang et al. (2024b). They steered the attention of pretrained language models to emphasize user-specified portions of user instructions, enabling models to follow instructions without explicit instruction fine-tuning. In our setting, we increase the attention weights of instruction-finetuned models on the entire user input prompt, which consequently decreases weights on other tokens (chat template role tokens, BOS/EOS tokens, and partially generated model responses). Similar to Section 2.2, we select and steer the representative context retrieval head on each layer, which allocates the highest attention to user tokens. See a more detailed discussion about head and layer selection in Appendix B.3. We select the best intervention factor α for each model on NIH from the set $[0.01, 0.1, 0.3, 0.5, 0.7, 0.9]$.

Table 1: NIH and DROP performance with attention steering. DROP is a complicated reading comprehension task requiring discrete operations such as addition, sorting or counting on multiple pieces of information retrieved from the context. “Baseline” and “+ Attention Steering” are evaluated with chat templates. “w/o chat template” shows the NIH performance without the chat template for reference (same as the numbers reported in Figure 2).

Task	Capabilities	Model Name	Baseline	+ Attention Steering	w/o chat template
NIH	sentence retrieval	Llama-2-7B-Chat	0.9917	0.9935	0.9975
		Llama-2-13B-Chat	0.9207	0.9375	0.9578
QuAC	sentence retrieval reading comprehension	Llama-2-7B-Chat	0.1330	0.1340	-
		Llama-2-13B-Chat	0.1180	0.1230	-
DROP	retrieval math operation	Llama-2-7B-Chat	0.4422	0.4416	-
		Llama-2-13B-Chat	0.4620	0.4584	-

Post-hoc attention steering partially recovers the NIH performance but produces side effects. We report the performance of attention steering in Table 1. Attention steering requires customized attention calculations for different heads and layers, which limits the use of several existing efficient attention implementations. Therefore, we are only able to apply attention steering to two Llama-2 models with 4,000-token context windows. In addition to the NIH test, we report the performance on two additional contextual QA tasks: QuAC (Choi et al., 2018) and DROP (Dua et al., 2019). Unlike NIH and QuAC, which retrieve exact sentences from the context, DROP requires the model not only to understand and retrieve relevant information from the context but also to apply discrete mathematical operations to the retrieved information. As shown in the table, attention steering can boost performance on simple context retrieval tasks such as NIH and QuAC. However, on DROP, which requires a more complex combination of different capabilities, performance with attention steering is negatively impacted. The deteriorating performance on DROP suggests that intervening in attention scores to emphasize user tokens, while improving context awareness, might impair other capabilities of the model.

In the next section, we introduce a finetuning strategy to mitigate the loss of context awareness with less side effects.

3 Instruction Fine-tuning with Context-dependency Indicators

In this section, we propose a fine-tuning strategy to mitigate the aforementioned loss of context awareness associated with chat roles. Our approach is based on the intuition that the model learns the bias from instruction-tuning datasets, which contain examples that rely less on user-provided context. Therefore, if we can identify “context-dependent” examples from these instruction fine-tuning datasets, we can apply several strategies — such as data augmentation, data selection, and conditional fine-tuning—to encourage the model to focus more on user-provided context.

In Section 3.1, we propose an attention-based metric to identify context-dependent examples from general instruction fine-tuning datasets. In Section 3.2, we apply conditional fine-tuning and add an indicator to each identified “context-dependent” instruction during instruction fine-tuning. In this way, the model is encouraged to focus more on user-provided context when it encounters the indicator during inference.

3.1 Identifying context-dependent Instructions

A training sample in the instruction fine-tuning dataset is a conversation between the user and model assistant, which may consist of multiple instruction-response pairs. Formally, we denote user instructions as X , assistant responses as Y , and a conversation of n total turns as $C = [X_1, Y_1, \dots, X_n, Y_n]$.

Identifying context-dependent instructions with a reference language model. To identify context-dependent instructions, we start by preparing a seed instruction fine-tuned model M , which can be the same or a weaker pretrained model fine-tuned with the original instruction fine-tuning dataset. We then define the context-dependency score for the m^{th} turn response Y_m given its instruction \mathbf{X}_m and conversation history:

$$s_M(\mathbf{Y}_m) = \frac{1}{|\mathbf{Y}_m|} \sum_{\mathbf{y} \in \mathbf{Y}_m} \max_{h \in H} \left(\sum_{\mathbf{x} \in \mathbf{X}_1 \cup \dots \cup \mathbf{X}_m} \text{Att}_h(\mathbf{y}, \mathbf{x}) \right), \quad (2)$$

where H is the set of attention heads in model M and $\text{Att}(\mathbf{y}, \mathbf{x})$ is the attention weight from token \mathbf{y} to \mathbf{x} . Intuitively, the score $s_M(\mathbf{Y}_m)$ measures the sum of attention scores allocated to all user instructions in prior turns $\mathbf{X}_1 \cup \dots \cup \mathbf{X}_m$, averaged over response tokens $\mathbf{y} \in \mathbf{Y}_m$. As different heads learn different capabilities, we calculate the score on the most representative head for context retrieval on each layer, specifically the head that allocates the highest attention weight to user tokens. For practical efficiency, we compute the score on a single middle layer. We defer the discussion of layer and head selection to Appendix B.4.

3.2 Instruction Fine-tuning with Context-dependency Indicators

A threshold $0 < \beta < 1$ can be selected after the context-dependency score is obtained for each instruction-response pair. A conversation turn $(\mathbf{X}_m, \mathbf{Y}_m)$ with $s_M(\mathbf{Y}_m) > \beta$ is considered context-dependent. We append a special token `[IND]` to the user instruction \mathbf{X}_m if it is context-dependent. In our implementation, the special token `[IND]` is added as an additional special token to the vocabulary to avoid conflicts with existing ones.

Our method is more general in terms of task and input format compared to related works, which synthesize context-dependent examples targeted toward specific tasks (e.g., contextual QA) (An et al., 2024). This makes our method more applicable to different types of user queries that require greater attention to user-provided context.

After conditional instruction fine-tuning, the user can specify whether to add this indicator to their query, depending on whether the model response should rely more on user-provided context.

4 Experiments

We validate the effectiveness of our method using three open-source pretrained models and a set of context-dependent and general tasks. Our results demonstrate that this method improves performance on context-dependent tasks compared to vanilla finetuning, while maintaining instruction-following performance on general tasks.

4.1 Experimental Settings

4.1.1 Models

We evaluate our method on three open-source pretrained large language models: TinyLlama-1.1B (Zhang et al., 2024a), Llama-2-7B (Touvron et al., 2023), and Llama-3-8B (Dubey et al., 2024). TinyLlama-1.1B is a 1.1B Llama

Table 2: Statistics of instruction fine-tuning datasets in our experiments. # denotes the number of conversations and individual instructions in the dataset. We report the statistics after performing preprocessing as detailed in Section 4.1.2. Average length is measured in the number of tokens with TinyLlama tokenization.

Datasets	Avg. conversation length	# conversations	# instructions
ShareGPT	1,567.68	93,645	331,722
UltraChat-200k	1,437.33	207,865	657,794
WizardLM-70K	484.00	57,523	57,523

model pretrained on 3 trillion tokens with a context window length of 2048. Llama-2-7B and Llama-3-8B have context windows of 4096 and 8192 tokens, respectively. Due to limited computational resources in academic labs, we are able to fine-tune only models with up to 8B parameters. We also truncate the training examples to 4096 tokens. We fine-tune Llama-2 and Llama-3 models using QLoRA (Dettmers et al., 2024) on transformer layers. Detailed hyperparameters can be found in Appendix A.1.1.

4.1.2 Instruction Fine-tuning Datasets

We experiment with three popular open-source instruction fine-tuning datasets: ShareGPT, adopted by Vicuna (Chiang et al., 2023), UltraChat-200k (Ding et al., 2023), and WizardLM-70K (Xu et al., 2023a). For ShareGPT, we follow the same preprocessing process as Chiang et al. (2023). We remove refusal responses from ShareGPT and WizardLM-70K to prevent the fine-tuned models from becoming oversensitive and frequently refusing to respond. For all three datasets, we remove model responses from incomplete conversation chunks that lack user input instructions. Statistics of the processed datasets are presented in Table 2.

4.1.3 Benchmarks and Metrics

Context awareness benchmarks. In addition to NIH, we report the performance on three closed-book QA tasks to benchmark context awareness: SQuAD (Rajpurkar et al., 2016), QuAC (Choi et al., 2018), and DROP (Dua et al., 2019). SQuAD is a reading comprehension benchmark where the answer to each question can be found in the context. We evaluate only the answerable subset of questions in SQuAD 1.0. QuAC is similar to SQuAD, but its questions are more open-ended and the lengths of the answers are longer. While NIH, SQuAD and QuAC only require direct retrieval from context, DROP requires a more comprehensive understanding and analysis of the given context and the answers require retrieval of multiple information from the context and discrete operations such as addition, sorting, or counting.

As instruction fine-tuned models are not specifically trained on QA tasks to provide concise answers, their responses are generally more verbose. Therefore, we report the containment score, defined as whether the model response contains the ground-truth answer, rather than the F1 score to exclude the effects of different models’ response styles. Prompt templates for QA tasks are listed in Appendix A.3.

For Needle-in-a-haystack, we report the recall error defined in Section 2.1, which is also the default metric used in Dubey et al. (2024). We set the maximum NIH context length to 1,000 for models fine-tuned on WizardLM-70K due to its shorter instruction lengths. For models fine-tuned on ShareGPT and UltraChat-200K, we set the maximum NIH context length to the maximum context window considered in fine-tuning, which is 2,000 for TinyLlama and 4,000 for Llama-2 / Llama-3. The prompt template used in NIH is the same as Section 2.1 except that we remove the response prefix and keep only the user input prompt.

General instruction-following benchmarks. To validate that our method maintains strong performance on general instruction-following tasks, we evaluate the fine-tuned models on MT-Bench (Zheng et al., 2023) where the response quality is rated by a GPT-4 judge based on helpfulness, relevance, accuracy, depth, creativity, and level of detail. We report the average rating across the MT-Bench test cases.

4.2 Instruction Fine-tuning with Context-dependency Indicators

Settings and hyperparameters. We adopt a TinyLlama model finetuned on the original ShareGPT (Vicuna) dataset as the seed model M . We compute the context-dependency score on a middle layer (15 in all of our main experiments) for faster computation. As we show in Appendix B.4, subsets selected by scores calculated on different middle layers are highly consistent. We set the threshold for context-awareness as $\beta = 0.6$ for all experiments reported in Table 4. An ablation study on the choice of threshold value can be found in Appendix B.5.

Table 3: Ratio of identified context-dependent instructions in each instruction finetuning dataset. Total number of instructions in each dataset can be found in Table 2

Dataset	0.5	0.6	0.7	0.8
ShareGPT (Vicuna)	0.14	0.10	0.07	0.04
UltraCHat-200K	0.22	0.18	0.14	0.11
WizardLM-70K	0.34	0.23	0.13	0.06

Table 4: Comparing vanilla instruction finetuning with finetuning with context-relevant indicators (+ indicator). On ‘+ Indicator’ models, `[IND]` is added in all evaluations. As a reference, we also list the performances evaluated on official Llama-2 and Llama-3 instruct models, which are finetuned with closed-source datasets.

SFT dataset	Pretrained Model	Method	NIH	SQuAD	QuAC	DROP	Avg.	MT-Bench
ShareGPT (Vicuna)	TinyLlama-1.1B	Vanilla	0.9846	0.5918	0.1130	0.2739	0.4908	3.7250
	TinyLlama-1.1B	+ Indicator	0.9921	0.6144	0.1290	0.2784	0.5035	3.7375
	Llama-2-7b	Vanilla	0.3378	0.7601	0.1590	0.3390	0.3990	6.4875
	Llama-2-7b	+ Indicator	0.7007	0.7830	0.1600	0.3390	0.4957	5.7375
	Llama-3-8b	Vanilla	0.8957	0.8216	0.1560	0.4215	0.5737	7.4375
	Llama-3-8b	+ Indicator	0.9404	0.8394	0.1660	0.4317	0.5943	7.1625
UltraChat-200K	TinyLlama-1.1B	Vanilla	1.0	0.7289	0.1520	0.3096	0.5476	3.9000
	TinyLlama-1.1B	+ Indicator	1.0	0.7475	0.1570	0.3096	0.5535	4.1125
	Llama-2-7b	Vanilla	0.9850	0.8272	0.1540	0.3791	0.5863	5.7125
	Llama-2-7b	+ Indicator	0.9725	0.8508	0.1570	0.3758	0.5890	5.8125
	Llama-3-8b	Vanilla	1.0	0.8393	0.1610	0.5099	0.6276	7.2375
	Llama-3-8b	+ Indicator	1.0	0.8510	0.1660	0.5022	0.6298	6.8500
WizardLM-70K	TinyLlama-1.1B	Vanilla	0.9250	0.5994	0.0990	0.2753	0.4747	4.2750
	TinyLlama-1.1B	+ Indicator	0.9925	0.6279	0.1140	0.2836	0.5045	4.3000
	Llama-2-7b	Vanilla	0.7375	0.8229	0.1550	0.3407	0.5140	5.7750
	Llama-2-7b	+ Indicator	0.9254	0.8260	0.1640	0.3444	0.5650	6.2250
	Llama-3-8b	Vanilla	0.9846	0.8765	0.1560	0.4687	0.6215	7.1125
	Llama-3-8b	+ Indicator	0.9871	0.8792	0.1710	0.4785	0.6290	7.5250
(Closed-source datasets)	Llama-2-7b-chat	-	0.8264*	0.8301	0.1330	0.4422	0.5579	6.9375
	Llama-3-8b-Instruct	-	1.0*	0.8612	0.1850	0.4654	0.6279	8.0750

* Here NIH is evaluated without the response prefix used in Section 2.1 and the maximum context length is set to 4096 for fair comparison. Therefore, the numbers are different from the numbers in Figure 2.

Sparsity of context-dependent instructions. We compute the context-dependency scores on all three instruction fine-tuning datasets and report the ratio of identified context-dependent instructions with different threshold values β in Table 3. Context-dependent instructions are rare in all three instruction fine-tuning datasets. This observation supports our hypothesis that the model learns an attention bias from the instruction dataset to weigh user tokens less importantly.

Conditional finetuning improves performance on context-dependent tasks. We report the performance of NIH and three contextual QA tasks in Table 4. For the “vanilla” fine-tuning setting, we train and evaluate the model without the indicator token. For the “+ Indicator” setting, we add the indicator token to the selected subset of prompts in finetuning and all queries for evaluation. According to the table, “+ Indicator” outperforms “vanilla” fine-tuning in most cases. Particularly, “+ Indicator” outperforms vanilla finetuning on DROP for most cases, confirming that the training-time solution handles trade-offs between language model capabilities well. The results demonstrate that models can learn to focus more on the user-provided context when the indicator token is present in the prompt.

Conditional finetuning maintains the performance on general instruction-following. We report the evaluation results on MT-Bench in Table 4 as an evaluation for general instruction-following. Indicators are presented during evaluation by default. Models fine-tuned with our method demonstrate comparable or even better performance on MT-Bench in most cases. Notably, MT-Bench performance increases on datasets with more context-dependent conversations (such as WizardLM-70K), which is expected when the context-dependent subset becomes more diverse.

Therefore, our methods can effectively mitigate the loss of context awareness without losing the general ability to follow instructions.

5 Related Work

Instruction fine-tuning and chat templates. Large language models only learn language modeling on general corpus during pretraining. To enable instruction-following, they usually require supervised fine-tuning on instruction-following datasets (SFT) (Wei et al., 2021; Ouyang et al., 2022), followed by reinforcement learning with human feedback (RLHF) (Christiano et al., 2017). In this paper, we mainly focus on the SFT stage. Instruction fine-tuning datasets consist of user instruction and target model response pairs, which can be collected from modified NLP tasks (Wei et al., 2021; Longpre et al., 2023), human annotations (Ouyang et al., 2022; Chiang et al., 2023) or synthesized data from existing LLMs (Ding et al., 2023; Xu et al., 2023a). Instruction fine-tuning usually converts training examples into a dialog format with a chat template, which consists of a user role indicator (e.g. `[INST]` in llama-2 models), an assistant role indicator (e.g. `[/INST]` in llama-2 models) and an optional system role indicator (e.g. `<<SYS>>` in llama-2 models). Other role indicators are also used in more complicated scenarios such as tool using (Schick et al., 2023). However, these role indicators and role partition in the conversation are not sufficiently presented and learned during pretraining, making them prone to bias during fine-tuning.

Context awareness and hallucinations in Large Language Models In this work, we define context awareness as the capability of large language models to retrieve and understand information from user-provided context and respond accordingly. Context awareness is crucial for mitigating hallucinations where the response is not consistent with the provided context, such as the “closed-domain” hallucination in Ouyang et al. (2022) and intrinsic hallucination in Huang et al. (2023). Several existing works aim to understand and mitigate these intrinsic hallucinations. Liu et al. (2024) studies the failure of context retrieval when the relevant information is in the middle of the provided context, showing the existence of positional bias in context retrieval. Follow-up work (Hsieh et al., 2024) proposes to calibrate this positional bias and mitigate the issue. In our work, we study a new **role bias** in popular open-source instruction-finetuned models, where the context receives less attention when marked as user tokens by the chat template.

Side effects of instruction finetuning Neural networks are known to easily forget existing knowledge or capabilities when continually trained on a new task or domain, which is called catastrophic forgetting in existing works (Kirkpatrick et al., 2017). However, it is commonly believed that traditional catastrophic forgetting on pretraining-stage capabilities can be significantly mitigated by finetuning the model on a diversified mixture of prompts (Longpre et al., 2023; Bai et al., 2022; Glaese et al., 2022). Another well-known side effect is reward hacking in RLHF, where the models utilize short-cuts in an imperfect reward model during training instead of learning the target task. Reward hacking in RLHF can lead to a divergence of the model behavior from the optimal one, with issues such as format overfitting (Singhal et al., 2023; Wang et al., 2023).

6 Conclusion

This work highlights the detrimental effects of supervised instruction fine-tuning on the context awareness of pre-trained language models, even in scenarios involving short context lengths. We have identified that the decline in context awareness is closely linked to attention allocation biases within chat templates, which are learned during conversational instruction finetuning. To address this issue, we first propose a quantitative metric to identify context-dependent instructions from the general instruction finetuning dataset. We then propose a training-time approach that employs conditional indicators to signal these instructions during the instruction-tuning process. Our method effectively maintains contextual understanding while benefiting from supervised instruction.

Limitation First of all, due to computational resource limitations, our methods were only validated on smaller-sized models ($\leq 7B$) with QLoRA (Dettmers et al., 2024). We hope to extend the experiments to full finetuning or larger models when more resources become available. Second, our technique of associating context-dependent user instructions with the indicator token may also encode other unintended styles from the selected subset of instructions. This issue is particularly aggravated when the subset of context-relevant samples is small and significantly different from the remaining dataset. One future direction is to better disentangle the context-dependency signal within the selected corpus. Finally, utilizing the indicator token requires users to know which instructions would benefit from more emphasis on the user context. Tasks demonstrated in our experiment (e.g., keyword retrieval and closed-book QA) evidently require more attention to the user context. However, complex tasks may involve multiple language skills, which complicates whether applying the indicator token will benefit the performance. A future direction is to automatically determine when to append the indicator.

References

Rishabh Agarwal, Avi Singh, Lei M. Zhang, Bernd Bohnet, Luis Rosias, Stephanie Chan, Biao Zhang, Ankesh Anand, Zaheer Abbas, Azade Nova, John D. Co-Reyes, Eric Chu, Feryal Behbahani, Aleksandra Faust, and Hugo Larochelle. Many-shot in-context learning, 2024. URL <https://arxiv.org/abs/2404.11018>.

Shengnan An, Zexiong Ma, Zeqi Lin, Nanning Zheng, and Jian-Guang Lou. Make your llm fully utilize the context, 2024. URL <https://arxiv.org/abs/2404.16811>.

Yuntao Bai, Andy Jones, Kamal Ndousse, Amanda Askell, Anna Chen, Nova DasSarma, Dawn Drain, Stanislav Fort, Deep Ganguli, Tom Henighan, et al. Training a helpful and harmless assistant with reinforcement learning from human feedback. *arXiv preprint arXiv:2204.05862*, 2022.

Wei-Lin Chiang, Zhuohan Li, Zi Lin, Ying Sheng, Zhanghao Wu, Hao Zhang, Lianmin Zheng, Siyuan Zhuang, Yonghao Zhuang, Joseph E. Gonzalez, Ion Stoica, and Eric P. Xing. Vicuna: An open-source chatbot impressing gpt-4 with 90%* chatgpt quality, March 2023. URL <https://lmsys.org/blog/2023-03-30-vicuna/>.

Eunsol Choi, He He, Mohit Iyyer, Mark Yatskar, Wen tau Yih, Yejin Choi, Percy Liang, and Luke Zettlemoyer. Quac : Question answering in context, 2018. URL <https://arxiv.org/abs/1808.07036>.

Paul F Christiano, Jan Leike, Tom Brown, Miljan Martic, Shane Legg, and Dario Amodei. Deep reinforcement learning from human preferences. *Advances in neural information processing systems*, 30, 2017.

Tim Dettmers, Artidoro Pagnoni, Ari Holtzman, and Luke Zettlemoyer. Qlora: Efficient finetuning of quantized llms. *Advances in Neural Information Processing Systems*, 36, 2024.

Ning Ding, Yulin Chen, Bokai Xu, Yujia Qin, Zhi Zheng, Shengding Hu, Zhiyuan Liu, Maosong Sun, and Bowen Zhou. Enhancing chat language models by scaling high-quality instructional conversations. *arXiv preprint arXiv:2305.14233*, 2023.

Dheeru Dua, Yizhong Wang, Pradeep Dasigi, Gabriel Stanovsky, Sameer Singh, and Matt Gardner. DROP: A reading comprehension benchmark requiring discrete reasoning over paragraphs. In Jill Burstein, Christy Doran, and Thamar Solorio (eds.), *Proceedings of the 2019 Conference of the North American Chapter of the Association for Computational Linguistics: Human Language Technologies, Volume 1 (Long and Short Papers)*, pp. 2368–2378, Minneapolis, Minnesota, June 2019. Association for Computational Linguistics. doi: 10.18653/v1/N19-1246. URL <https://aclanthology.org/N19-1246>.

Abhimanyu Dubey, Abhinav Jauhri, Abhinav Pandey, Abhishek Kadian, Ahmad Al-Dahle, Aiesha Letman, Akhil Mathur, Alan Schelten, Amy Yang, Angela Fan, Anirudh Goyal, Anthony Hartshorn, Aobo Yang, Archi Mitra, Archie Sravankumar, Artem Korenev, Arthur Hinsvark, Arun Rao, Aston Zhang, Aurelien Rodriguez, Austen Gregerson, Ava Spataru, Baptiste Roziere, Bethany Biron, Binh Tang, Bobbie Chern, Charlotte Caucheteux, Chaya Nayak, Chloe Bi, Chris Marra, Chris McConnell, Christian Keller, Christophe Touret, Chunyang Wu, Corinne Wong, Cristian Canton Ferrer, Cyrus Nikolaidis, Damien Allonsius, Daniel Song, Danielle Pintz, Danny Livshits, David Esiobu, Dhruv Choudhary, Dhruv Mahajan, Diego Garcia-Olano, Diego Perino, Dieuwke Hupkes, Egor Lakomkin, Ehab AlBadawy, Elina Lobanova, Emily Dinan, Eric Michael Smith, Filip Radenovic, Frank Zhang, Gabriel Synnaeve, Gabrielle Lee, Georgia Lewis Anderson, Graeme Nail, Gregoire Mialon, Guan Pang, Guillem Cucurell, Hailey Nguyen, Hannah Korevaar, Hu Xu, Hugo Touvron, Iliyan Zarov, Imanol Arrieta Ibarra, Isabel Kloumann, Ishan Misra, Ivan Evtimov, Jade Copet, Jaewon Lee, Jan Geffert, Jana Vranes, Jason Park, Jay Mhadeokar, Jeet Shah, Jelmer van der Linde, Jennifer Billock, Jenny Hong, Jenya Lee, Jeremy Fu, Jianfeng Chi, Jianyu Huang, Jiawen Liu, Jie Wang, Jiecao Yu, Joanna Bitton, Joe Spisak, Jongsoo Park, Joseph Rocca, Joshua Johnstun, Joshua Saxe, Junteng Jia, Kalyan Vasuden Alwala, Kartikeya Upasani, Kate Plawiak, Ke Li, Kenneth Heafield, Kevin Stone, Khalid El-Arini, Krithika Iyer, Kshitiz Malik, Kuenley Chiu, Kunal Bhalla, Lauren Rantala-Yeary, Laurens van der Maaten, Lawrence Chen, Liang Tan, Liz Jenkins, Louis Martin, Lovish Madaan, Lubo Malo, Lukas Blecher, Lukas Landzaat, Luke de Oliveira, Madeline Muzzi, Mahesh Pasupuleti, Mannat Singh, Manohar Paluri, Marcin Kardas, Mathew Oldham, Mathieu Rita, Maya Pavlova, Melanie Kambadur, Mike Lewis, Min Si, Mitesh Kumar Singh, Mona Hassan, Naman Goyal, Narjes Torabi, Nikolay Bashlykov, Nikolay Bogoychev, Niladri Chatterji, Olivier Duchenne, Onur Çelebi, Patrick Alrassy, Pengchuan Zhang, Pengwei Li, Petar Vasic, Peter Weng, Prajwal Bhargava, Pratik Dubal, Praveen Krishnan, Punit Singh Koura, Puxin Xu, Qing He, Qingxiao Dong, Ragavan Srinivasan, Raj Ganapathy, Ramon Calderer, Ricardo Silveira Cabral, Robert Stojnic, Roberta Raileanu, Rohit Girdhar, Rohit Patel, Romain Sauvestre, Ronnie Polidoro, Roshan Sumbaly, Ross Taylor, Ruan Silva, Rui Hou, Rui Wang, Saghar Hosseini, Sahana Chennabasappa, Sanjay Singh, Sean Bell, Seohyun Sonia Kim, Sergey Edunov, Shaoliang Nie, Sharan Narang, Sharath Raparthy, Sheng Shen, Shengye Wan, Shruti Bhosale, Shun Zhang, Simon Vandenhende, Soumya Batra, Spencer Whitman, Sten Sootla, Stephane Collot, Suchin Gururangan, Sydney Borodinsky, Tamar Herman, Tara Fowler, Tarek Sheasha, Thomas Georgiou, Thomas Scialom, Tobias Speckbacher, Todor Mihaylov, Tong Xiao, Ujjwal Karn, Vedanuj Goswami, Vibhor Gupta, Vignesh Ramamathan, Viktor Kerkez, Vincent Gonguet, Virginie Do, Vish Vogeti, Vladan Petrovic, Weiwei Chu, Wenhan

Xiong, Wenyin Fu, Whitney Meers, Xavier Martinet, Xiaodong Wang, Xiaoqing Ellen Tan, Xinfeng Xie, Xuchao Jia, Xuewei Wang, Yaelle Goldschlag, Yashesh Gaur, Yasmine Babaei, Yi Wen, Yiwen Song, Yuchen Zhang, Yue Li, Yuning Mao, Zacharie Delpierre Coudert, Zheng Yan, Zhengxing Chen, Zoe Papakipos, Aaditya Singh, Aaron Grattafiori, Abha Jain, Adam Kelsey, Adam Shajnfeld, Adithya Gangidi, Adolfo Victoria, Ahuva Goldstand, Ajay Menon, Ajay Sharma, Alex Boesenberg, Alex Vaughan, Alexei Baevski, Allie Feinstein, Amanda Kallet, Amit Sangani, Anam Yunus, Andrei Lupu, Andres Alvarado, Andrew Caples, Andrew Gu, Andrew Ho, Andrew Poulton, Andrew Ryan, Ankit Ramchandani, Annie Franco, Aparajita Saraf, Arkabandhu Chowdhury, Ashley Gabriel, Ashwin Bharambe, Assaf Eisenman, Azadeh Yazdan, Beau James, Ben Maurer, Benjamin Leonhardi, Bernie Huang, Beth Loyd, Beto De Paola, Bhargavi Paranjape, Bing Liu, Bo Wu, Boyu Ni, Braden Hancock, Bram Wasti, Brandon Spence, Brani Stojkovic, Brian Gamido, Britt Montalvo, Carl Parker, Carly Burton, Catalina Mejia, Changhan Wang, Changkyu Kim, Chao Zhou, Chester Hu, Ching-Hsiang Chu, Chris Cai, Chris Tindal, Christoph Feichtenhofer, Damon Civin, Dana Beaty, Daniel Kreymer, Daniel Li, Danny Wyatt, David Adkins, David Xu, Davide Testuggine, Delia David, Devi Parikh, Diana Liskovich, Didem Foss, Dingkang Wang, Duc Le, Dustin Holland, Edward Dowling, Eissa Jamil, Elaine Montgomery, Eleonora Presani, Emily Hahn, Emily Wood, Erik Brinkman, Esteban Arcuate, Evan Dunbar, Evan Smothers, Fei Sun, Felix Kreuk, Feng Tian, Firat Ozgenel, Francesco Caggioni, Francisco Guzmán, Frank Kanayet, Frank Seide, Gabriela Medina Florez, Gabriella Schwarz, Gada Badeer, Georgia Swee, Gil Halpern, Govind Thatte, Grant Herman, Grigory Sizov, Guangyi, Zhang, Guna Lakshminarayanan, Hamid Shojanazeri, Han Zou, Hannah Wang, Hanwen Zha, Haroun Habeeb, Harrison Rudolph, Helen Suk, Henry Aspegren, Hunter Goldman, Ibrahim Damlaj, Igor Molybog, Igor Tufanov, Irina-Elena Veliche, Itai Gat, Jake Weissman, James Geboski, James Kohli, Japhet Asher, Jean-Baptiste Gaya, Jeff Marcus, Jeff Tang, Jennifer Chan, Jenny Zhen, Jeremy Reizenstein, Jeremy Teboul, Jessica Zhong, Jian Jin, Jingyi Yang, Joe Cummings, Jon Carvill, Jon Shepard, Jonathan McPhie, Jonathan Torres, Josh Ginsburg, Junjie Wang, Kai Wu, Kam Hou U, Karan Saxena, Karthik Prasad, Kartikay Khandelwal, Katayoun Zand, Kathy Matosich, Kaushik Veeraraghavan, Kelly Michelena, Keqian Li, Kun Huang, Kunal Chawla, Kushal Lakhota, Kyle Huang, Lailin Chen, Lakshya Garg, Lavender A, Leandro Silva, Lee Bell, Lei Zhang, Liangpeng Guo, Licheng Yu, Liron Moshkovich, Luca Wehrstedt, Madien Khabsa, Manav Avalani, Manish Bhatt, Maria Tsimpoukelli, Martynas Mankus, Matan Hasson, Matthew Lennie, Matthias Reso, Maxim Groshev, Maxim Naumov, Maya Lathi, Meghan Keneally, Michael L. Seltzer, Michal Valko, Michelle Restrepo, Mihir Patel, Mik Vyatskov, Mikayel Samvelyan, Mike Clark, Mike Macey, Mike Wang, Miquel Jubert Hermoso, Mo Metanat, Mohammad Rastegari, Munish Bansal, Nandhini Santhanam, Natascha Parks, Natasha White, Navyata Bawa, Nayan Singhal, Nick Egebo, Nicolas Usunier, Nikolay Pavlovich Laptev, Ning Dong, Ning Zhang, Norman Cheng, Oleg Chernoguz, Olivia Hart, Omkar Salpekar, Ozlem Kalinli, Parkin Kent, Parth Parekh, Paul Saab, Pavan Balaji, Pedro Rittner, Philip Bontrager, Pierre Roux, Piotr Dollar, Polina Zvyagina, Prashant Ratanchandani, Pritish Yuvraj, Qian Liang, Rachad Alao, Rachel Rodriguez, Rafi Ayub, Raghotham Murthy, Raghu Nayani, Rahul Mitra, Raymond Li, Rebekkah Hogan, Robin Battey, Rocky Wang, Rohan Maheswari, Russ Howes, Ruty Rinott, Sai Jayesh Bondu, Samyak Datta, Sara Chugh, Sara Hunt, Sargun Dhillon, Sasha Sidorov, Satadru Pan, Saurabh Verma, Seiji Yamamoto, Sharadh Ramaswamy, Shaun Lindsay, Shaun Lindsay, Sheng Feng, Sheng-hao Lin, Shengxin Cindy Zha, Shiva Shankar, Shuqiang Zhang, Shuqiang Zhang, Sinong Wang, Sneha Agarwal, Soji Sajuyigbe, Soumith Chintala, Stephanie Max, Stephen Chen, Steve Kehoe, Steve Satterfield, Sudarshan Govindaprasad, Sumit Gupta, Sungmin Cho, Sunny Virk, Suraj Subramanian, Sy Choudhury, Sydney Goldman, Tal Remez, Tamar Glaser, Tamara Best, Thilo Kohler, Thomas Robinson, Tianhe Li, Tianjun Zhang, Tim Matthews, Timothy Chou, Tzook Shaked, Varun Vontimitta, Victoria Ajayi, Victoria Montanez, Vijai Mohan, Vinay Satish Kumar, Vishal Mangla, Vítor Albiero, Vlad Ionescu, Vlad Poenaru, Vlad Tiberiu Mihailescu, Vladimir Ivanov, Wei Li, Wencheng Wang, Wenwen Jiang, Wes Bouaziz, Will Constable, Xiaocheng Tang, Xiaofang Wang, Xiao-jian Wu, Xiaolan Wang, Xide Xia, Xilun Wu, Xinbo Gao, Yanjun Chen, Ye Hu, Ye Jia, Ye Qi, Yenda Li, Yilin Zhang, Ying Zhang, Yossi Adi, Youngjin Nam, Yu, Wang, Yuchen Hao, Yundi Qian, Yuzi He, Zach Rait, Zachary DeVito, Zef Rosnbrick, Zhaoduo Wen, Zhenyu Yang, and Zhiwei Zhao. The llama 3 herd of models, 2024. URL <https://arxiv.org/abs/2407.21783>.

Tingchen Fu, Deng Cai, Lemao Liu, Shuming Shi, and Rui Yan. Disperse-then-merge: Pushing the limits of instruction tuning via alignment tax reduction. In Lun-Wei Ku, Andre Martins, and Vivek Srikumar (eds.), *Findings of the Association for Computational Linguistics ACL 2024*, pp. 2967–2985, Bangkok, Thailand and virtual meeting, August 2024. Association for Computational Linguistics. doi: 10.18653/v1/2024.findings-acl.175. URL <https://aclanthology.org/2024.findings-acl.175>.

Amelia Glaese, Nat McAleese, Maja Trebacz, John Aslanides, Vlad Firoiu, Timo Ewalds, Maribeth Rauh, Laura Weidinger, Martin Chadwick, Phoebe Thacker, et al. Improving alignment of dialogue agents via targeted human judgements. *arXiv preprint arXiv:2209.14375*, 2022.

Cheng-Yu Hsieh, Yung-Sung Chuang, Chun-Liang Li, Zifeng Wang, Long Le, Abhishek Kumar, James Glass, Alexander Ratner, Chen-Yu Lee, Ranjay Krishna, et al. Found in the middle: Calibrating positional attention bias improves

long context utilization. In *Findings of the Association for Computational Linguistics ACL 2024*, pp. 14982–14995, 2024.

Lei Huang, Weijiang Yu, Weitao Ma, Weihong Zhong, Zhangyin Feng, Haotian Wang, Qianglong Chen, Weihua Peng, Xiaocheng Feng, Bing Qin, et al. A survey on hallucination in large language models: Principles, taxonomy, challenges, and open questions. *ACM Transactions on Information Systems*, 2023.

Gautier Izacard, Patrick Lewis, Maria Lomeli, Lucas Hosseini, Fabio Petroni, Timo Schick, Jane Dwivedi-Yu, Armand Joulin, Sebastian Riedel, and Edouard Grave. Atlas: Few-shot learning with retrieval augmented language models. *Journal of Machine Learning Research*, 24(251):1–43, 2023.

Greg Kamradt. Llmtest_needleinahaystack, November 2023. URL https://github.com/gkamradt/LLMTest_NeedleInAHaystack.

Urvashi Khandelwal, Angela Fan, Dan Jurafsky, Luke Zettlemoyer, and Mike Lewis. Nearest neighbor machine translation. *arXiv preprint arXiv:2010.00710*, 2020.

James Kirkpatrick, Razvan Pascanu, Neil Rabinowitz, Joel Veness, Guillaume Desjardins, Andrei A Rusu, Kieran Milan, John Quan, Tiago Ramalho, Agnieszka Grabska-Barwinska, et al. Overcoming catastrophic forgetting in neural networks. *Proceedings of the national academy of sciences*, 114(13):3521–3526, 2017.

Yong Lin, Hangyu Lin, Wei Xiong, Shizhe Diao, Jianmeng Liu, Jipeng Zhang, Rui Pan, Haoxiang Wang, Wenbin Hu, Hanning Zhang, Hanze Dong, Renjie Pi, Han Zhao, Nan Jiang, Heng Ji, Yuan Yao, and Tong Zhang. Mitigating the alignment tax of rlhf, 2024. URL <https://arxiv.org/abs/2309.06256>.

Nelson F. Liu, Kevin Lin, John Hewitt, Ashwin Paranjape, Michele Bevilacqua, Fabio Petroni, and Percy Liang. Lost in the middle: How language models use long contexts. *Transactions of the Association for Computational Linguistics*, 12:157–173, 2024. doi: 10.1162/tacl_a_00638. URL <https://aclanthology.org/2024.tacl-1.9>.

Shayne Longpre, Le Hou, Tu Vu, Albert Webson, Hyung Won Chung, Yi Tay, Denny Zhou, Quoc V Le, Barret Zoph, Jason Wei, et al. The flan collection: Designing data and methods for effective instruction tuning. In *International Conference on Machine Learning*, pp. 22631–22648. PMLR, 2023.

Long Ouyang, Jeffrey Wu, Xu Jiang, Diogo Almeida, Carroll Wainwright, Pamela Mishkin, Chong Zhang, Sandhini Agarwal, Katarina Slama, Alex Ray, et al. Training language models to follow instructions with human feedback. *Advances in neural information processing systems*, 35:27730–27744, 2022.

Pranav Rajpurkar, Jian Zhang, Konstantin Lopyrev, and Percy Liang. Squad: 100,000+ questions for machine comprehension of text, 2016. URL <https://arxiv.org/abs/1606.05250>.

Timo Schick, Jane Dwivedi-Yu, Roberto Densi, Roberta Raileanu, Maria Lomeli, Eric Hambro, Luke Zettlemoyer, Nicola Cancedda, and Thomas Scialom. Toolformer: Language models can teach themselves to use tools. In *Thirty-seventh Conference on Neural Information Processing Systems*, 2023. URL <https://openreview.net/forum?id=Yacmpz84TH>.

Prasann Singhal, Tanya Goyal, Jiacheng Xu, and Greg Durrett. A long way to go: Investigating length correlations in rlhf. *arXiv preprint arXiv:2310.03716*, 2023.

Hugo Touvron, Louis Martin, Kevin Stone, Peter Albert, Amjad Almahairi, Yasmine Babaei, Nikolay Bashlykov, Soumya Batra, Prajjwal Bhargava, Shruti Bhosale, et al. Llama 2: Open foundation and fine-tuned chat models. *arXiv preprint arXiv:2307.09288*, 2023.

Yizhong Wang, Hamish Ivison, Pradeep Dasigi, Jack Hessel, Tushar Khot, Khyathi Chandu, David Wadden, Kelsey MacMillan, Noah A Smith, Iz Beltagy, et al. How far can camels go? exploring the state of instruction tuning on open resources. *Advances in Neural Information Processing Systems*, 36:74764–74786, 2023.

Jason Wei, Maarten Bosma, Vincent Y Zhao, Kelvin Guu, Adams Wei Yu, Brian Lester, Nan Du, Andrew M Dai, and Quoc V Le. Finetuned language models are zero-shot learners. *arXiv preprint arXiv:2109.01652*, 2021.

Wenhai Wu, Yizhong Wang, Guangxuan Xiao, Hao Peng, and Yao Fu. Retrieval head mechanistically explains long-context factuality, 2024. URL <https://arxiv.org/abs/2404.15574>.

Can Xu, Qingfeng Sun, Kai Zheng, Xiubo Geng, Pu Zhao, Jiazhan Feng, Chongyang Tao, and Dixin Jiang. Wizardlm: Empowering large language models to follow complex instructions. *arXiv preprint arXiv:2304.12244*, 2023a.

Peng Xu, Wei Ping, Xianchao Wu, Lawrence McAfee, Chen Zhu, Zihan Liu, Sandeep Subramanian, Evelina Bakhaturina, Mohammad Shoeybi, and Bryan Catanzaro. Retrieval meets long context large language models. *arXiv preprint arXiv:2310.03025*, 2023b.

Peiyuan Zhang, Guangtao Zeng, Tianduo Wang, and Wei Lu. Tinyllama: An open-source small language model, 2024a.

Qingru Zhang, Chandan Singh, Liyuan Liu, Xiaodong Liu, Bin Yu, Jianfeng Gao, and Tuo Zhao. Tell your model where to attend: Post-hoc attention steering for LLMs. In *The Twelfth International Conference on Learning Representations*, 2024b. URL <https://openreview.net/forum?id=xZDW00oejd>.

Lianmin Zheng, Wei-Lin Chiang, Ying Sheng, Siyuan Zhuang, Zhanghao Wu, Yonghao Zhuang, Zi Lin, Zhuohan Li, Dacheng Li, Eric P. Xing, Hao Zhang, Joseph E. Gonzalez, and Ion Stoica. Judging llm-as-a-judge with mt-bench and chatbot arena, 2023. URL <https://arxiv.org/abs/2306.05685>.

A Appendix

A.1 Experimental Details

A.1.1 Instruction Fine-tuning

We adopted the fine-tuning recipes from the Huggingface alignment-handbook² for Llama-2 and Llama-3 QLoRA tuning. For the TinyLlama model, we used the fine-tuning recipe provided by the author³. We finetuned the models for one epoch on ShareGPT and UltraChat-200K, and two epochs on WizardLM-70K due to its smaller training set. We used the TinyLlama chat template for all instruct models finetuned in Table 4.

A.2 NIH Evaluation Details

For all NIH evaluations, we average the recall error across 400 tests. Specifically, we evaluate on 20 context lengths uniformly distributed between 200 and the maximum context length, and 20 needle insertion depths uniformly located between 0% and 100%.

To ensure that our NIH evaluation is not sensitive to differences in prompt templates, we run evaluations with 4 different prompt templates on small-scale experiments and report the mean and standard deviation. For evaluations on larger models or larger context window sizes, we report the evaluation results using only one prompt template. We illustrate the mean errors in Figure 1. Complete results with standard deviations can be found in Table 7.

A.3 Contextual QA Evaluation Details

We list the prompts used in contextual QA tasks in Table 5 and Table 6. For contextual QA tasks, we generate answers of up to 100 tokens and truncate them at the end of the first complete sentence. For NIH tests, we generate answers of up to 50 tokens.

As UltraChat-200K constructs its data with a fixed set of prompt templates similar to our default ones used in evaluation (the templates used for ShareGPT and WizardLM models in Table 6 and 5), we evaluate UltraChat-200K-finetuned models with a simpler template to exclude the impact of overfitting on finetuning prompt templates.

Table 5: Prompt templates used for SQuAD and DROP in Table 1 and Table 4 when the model is finetuned on different instruction finetuning datasets.

Instruct Finetuning Dataset	Template for SQuAD and DROP
ShareGPT & WizardLM-70K UltraChat-200K	{context}\nAnswer the question according to the above passage: {question} {context} {question}

Table 6: Prompt templates used for QuAC in Table 1 and Table 4 when the model is finetuned on different instruction finetuning datasets.

Instruct Finetuning Dataset	Template for QuAC
ShareGPT & WizardLM-70K UltraChat-200K	{context}\nAnswer the question with pieces from the the above passage: {question} {context} {question}

B Additional Experiment Results

B.1 Full NIH Results on Open-source Official Models

In Figure 2, we only report the NIH performances when the response prefix is added, for fair comparison. In Table 7, we show the exact numbers for Figure 2 as well as additional evaluation results without the response prefix. When the response prefix is removed, the performance drop on NIH is even more significant compared to results without chat templates.

The standard deviations shown in the table are explained in Section A.2.

²<https://github.com/huggingface/alignment-handbook>

³<https://github.com/jzhang38/TinyLlama>

Table 7: NIH performance with and without chat templates on different models. The mean and standard deviations were calculated using 4 different prompt templates listed in Table 8.

Model Name	Context window	w/o chat template	w/ chat template	
		w/ response prefix	w/ response prefix	w/o response prefix
Llama-2-7b	4K	98.94 \pm 0.33%	-	-
Llama-2-7b-chat		99.40 \pm 0.48%	99.17 \pm 0.28 %	92.45 \pm 1.24%
Llama-2-13b	4K	98.89 \pm 0.34%	-	-
Llama-2-13b-chat		96.13 \pm 0.64%	91.50 \pm 0.76%	92.78 \pm 0.24%
Llama-3-8b	8K	99.62 \pm 0.26%	-	-
Llama-3-8b-instruct		99.92 \pm 0.09%	96.10 \pm 0.58%	95.89 \pm 0.62%
Llama-3.1-8b	128K	86.89%	-	-
Llama-3.1-8b-instruct		98.17%	95.64%	94.75%
mistral-v0.2	32K	100%	-	-
mistral-v0.2-instruct		99.00%	94.14%	93.92%
mistral-v0.3	32K	100%	-	-
mistral-v0.3-instruct		99.32%	84.71%	72.00%
gemma-2-9b	8K	100 \pm 0%	-	-
gemma-2-9b-it		98.75 \pm 0%	98.03 \pm 0%	98.72 \pm 0.54%
gemma-2-27b	8K	100%	-	-
gemma-2-27b-it		100%	99.64%	99.25%

Table 8: Four different prompt templates were used in the NIH evaluation. In Table 7, we report the mean and standard deviation across different prompt templates for small models and small context windows. {context} represents the context with the needle inserted.

Prompt templates in NIH evaluation
You are a helpful AI assistant that answers a question using only the provided document: {context}
Question: {retrieval_question}
You are a helpful AI assistant that answers a question using only the provided context: {context}
Question: {retrieval_question}
Document: {context}
Answer the question according to the provided document: {retrieval_question}
Context: {context}
Answer the question according to the provided context: {retrieval_question}

B.2 Full Results for Figure 2

In Figure 3, we only show the changes in attention allocation with and without chat templates. In Figure 4, we show the absolute numbers of attention allocation for each part of the input prompts. When the chat template is added, we normalize the attention weights on user tokens, response tokens, and the BOS token only, with the sum of attention allocation being 1.

B.3 Probing Context Retrieval Heads

In Sections 2.2, 2.3, and 3.1, we mentioned identifying a representative context retrieval head on each layer that allocates the largest attention to user tokens. Because different attention heads can have very different functionalities,

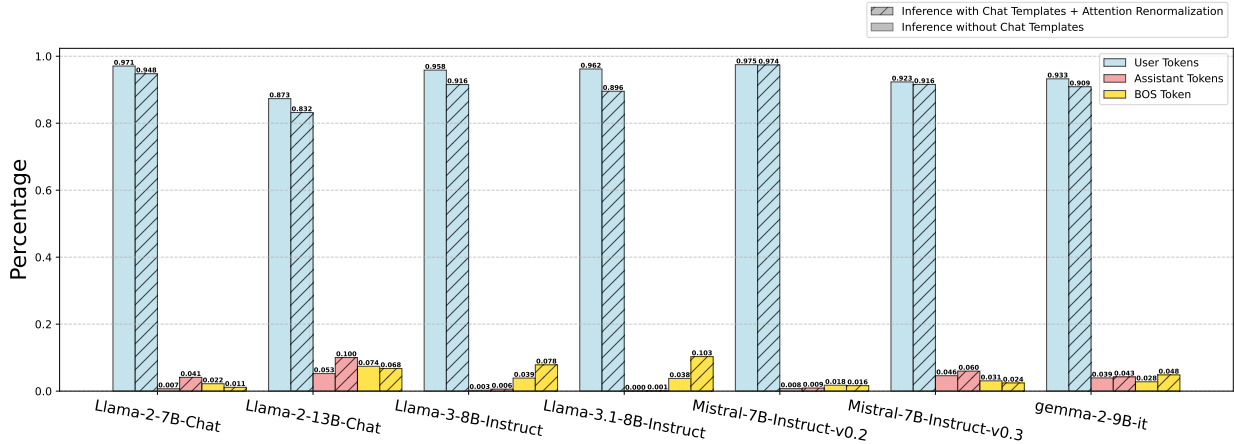


Figure 4: We visualize the full attention allocation on user tokens, assistant tokens, and BOS token with and without applying the chat templates. The attention allocation is calculated when the model is generating the first answer token in its response. For cases where the chat template is applied, we normalize the attention values on user tokens, assistant tokens, and the BOS token such that attention scores allocated to these three sum up to 1. The attention weights are averaged across 400 tests with context lengths ranging from 200 to 4000 and needle depths from 0% to 100%.

and context retrieval heads can be sparse among all heads (Wu et al., 2024), we believe that selecting a representative context retrieval head for visualization, attention steering, and data selection is both necessary and important. Specifically, given an input sequence $\mathbf{x}_1, \mathbf{x}_2, \dots, \mathbf{x}_m$ with m tokens, we select the context retrieval head h^* from each layer l that allocates the highest attention to user tokens when generating the first answer token:

$$h^* = \arg \max_{h \in H_l} \sum_{\mathbf{x}_i \in U} \text{Att}_{h,l}(\mathbf{x}_{-1}, \mathbf{x}_i) \quad (3)$$

, where \mathbf{x}_{-1} and \mathbf{x}_i are the last token and i th token in the sequence of tokens on each layer, respectively. U is a subset of all user tokens.

In Section 2.2, we select the retrieval head on layer 15 for each input prompt and visualize the average attention change on the selected head across different prompts. In Section 2.3, we select one retrieval head on each layer using a sampled NIH prompt and steer all identified retrieval heads. In Section 3.1, we select the retrieval head on layer 15 for each input prompt and calculate the context-dependency score. In Section B.4, we provide a further discussion on the agreement between different layers.

B.4 Agreement between Different Layers

In Figure 5, we calculate and visualize the disagreement heatmap in \hat{S} selection when the context-dependency score is calculated across different layers. We use the same TinyLlama model, finetuned on the vanilla ShareGPT dataset, as the seed model M . Specifically, we first calculate the context-dependency scores for each conversation turn in 500 randomly sampled examples from the ShareGPT dataset across different layers. We then select the top 10% of conversation turns with the highest context-dependency scores on each layer l as the subset \hat{S}_l . We compute the disagreement between two layers l and l' by calculating the ratio of non-overlapping conversation turns in their respective subsets \hat{S}_l and $\hat{S}_{l'}$. We can see from the figure that the disagreement among the 9 middle layers is low, indicating that we can safely choose an arbitrary layer for the context-dependency score calculation.

B.5 Ablation Study for Different Threshold β

We use $\beta = 0.6$ in all our main experiments. To evaluate the sensitivity to the threshold β , we select \hat{S} with different thresholds and prepare the final modified instruction finetuning dataset. We finetune a TinyLlama-1.1B model on these three datasets and evaluate it on three contextual QA tasks and MT-Bench. As shown in Table 9, all three models outperform vanilla finetuning on the contextual QA tasks. However, performance on MT-Bench shows a decreasing trend when the threshold increases from 0.5 to 0.7, potentially due to a more drastic difference between \hat{S} and the unselected subset.

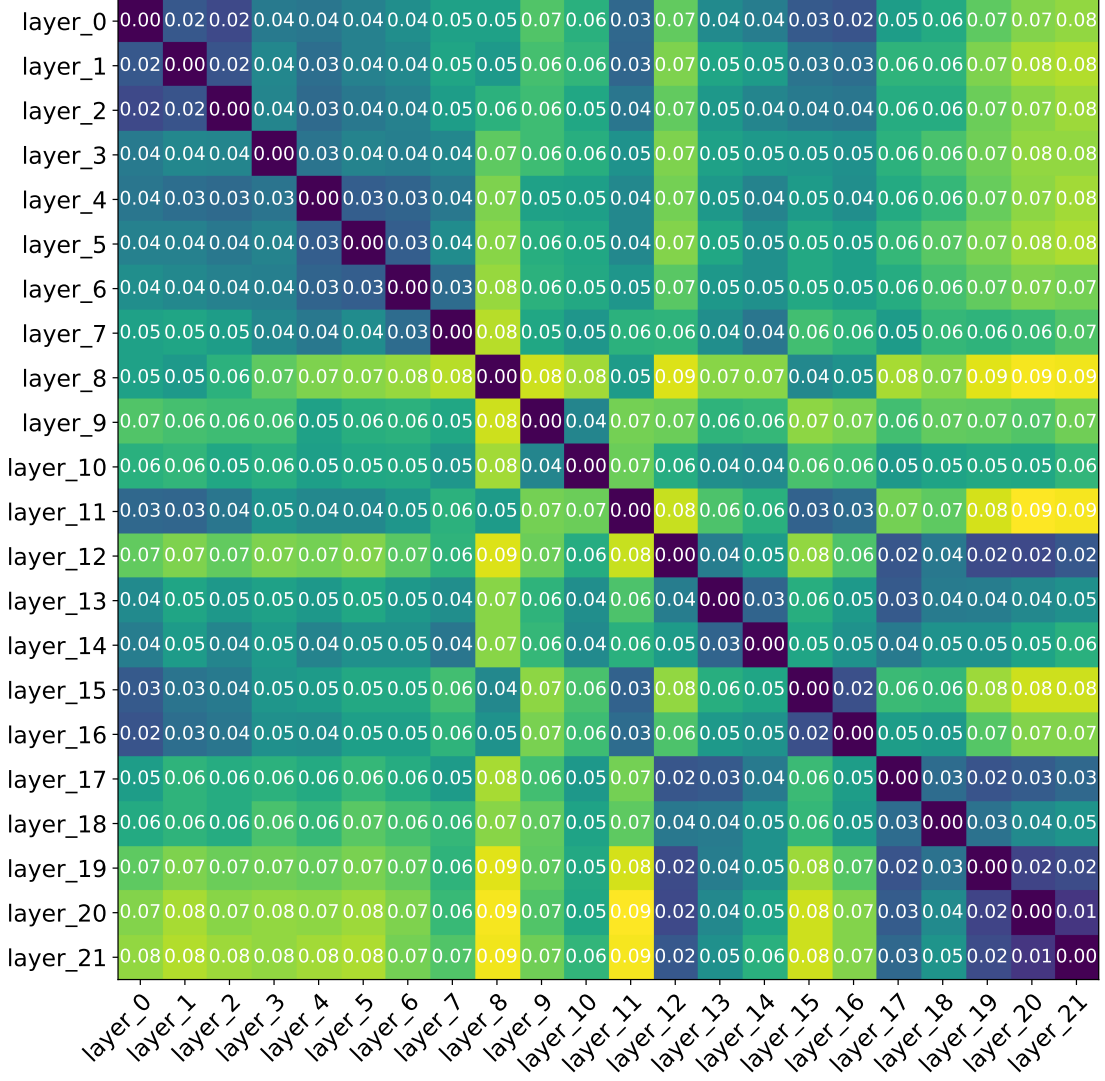


Figure 5: We visualize the disagreement heatmap of \hat{S} selection when the context-dependency score $S_M(\mathbf{Y}_m)$ is calculated across different layers. We select as \hat{S} the 10% of conversation turns with the highest context-dependency scores on each layer. The disagreement is measured by the number of non-overlapping conversation turns in \hat{S} selected by any two layers.

B.6 Distribution of Instruction Lengths

Here we visualize the changes in the distribution of instruction lengths between the original instruction finetuning dataset and the selected context-dependent subset \hat{S} . Although higher context-dependency is to some extent correlated with longer instruction lengths, there is still a large number of short instructions showing high context dependency and selected for inclusion in \hat{S} .

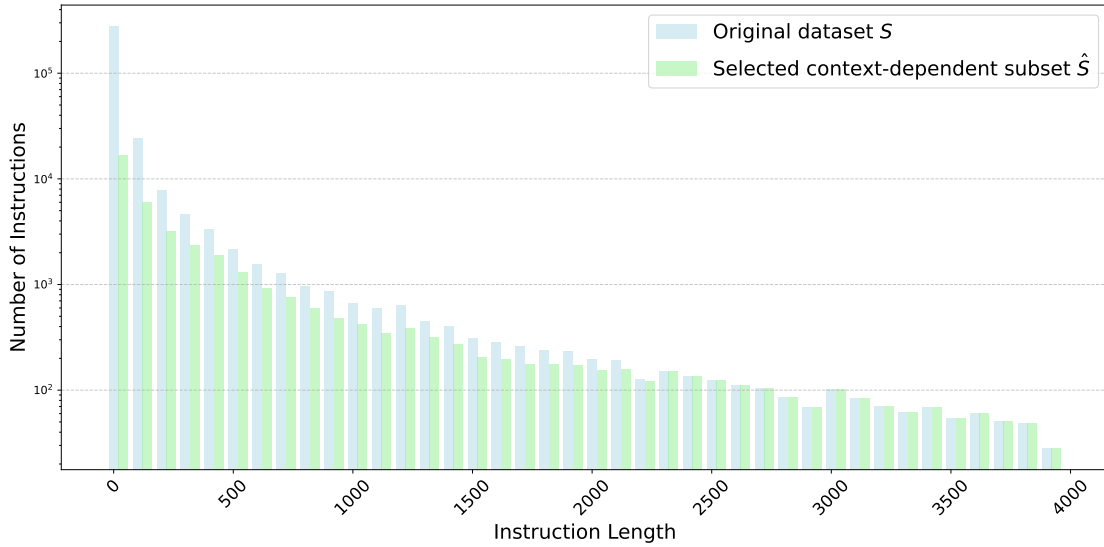


Figure 6: Change of instruction lengths between the original and the selected subset from ShareGPT dataset.

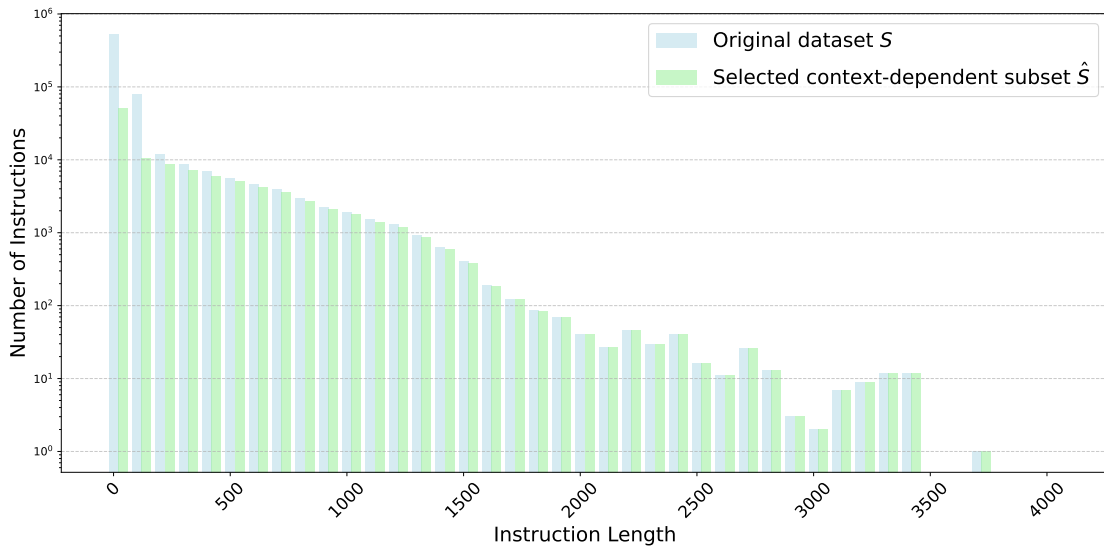


Figure 7: Change of instruction lengths between the original and the selected subset from UltraChat-200K dataset.

Table 9: Ablation study with different threshold β , which is used in Section 3.

Threshold β	SQuAD	QuAC	DROP	MT-Bench
1.0 (Vanilla)	0.5918	0.1130	0.2739	3.725
0.5	0.6207	0.1270	0.2872	4.075
0.6	0.6144	0.1290	0.2784	3.825
0.7	0.6160	0.1290	0.2786	3.675

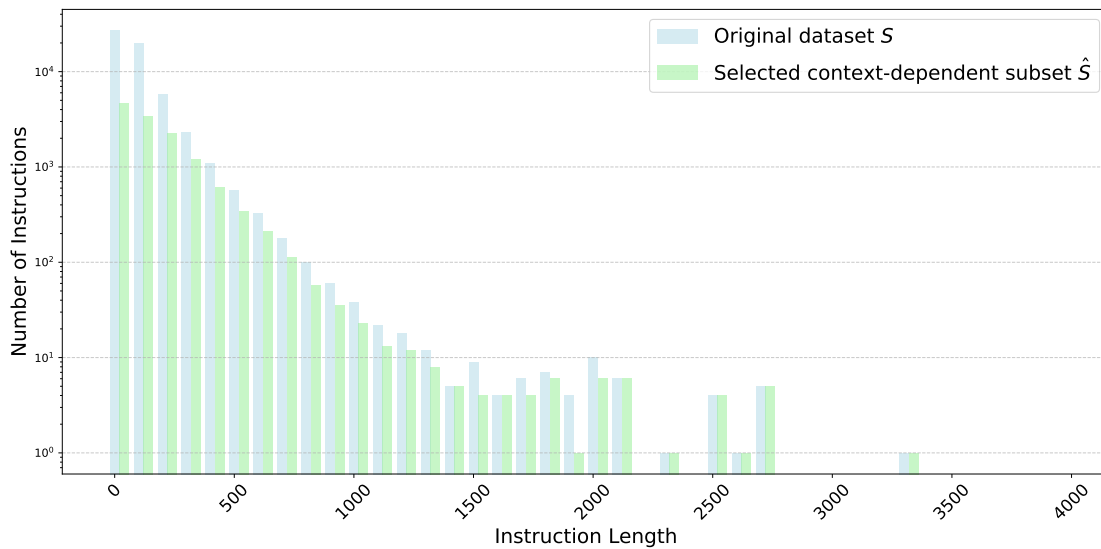


Figure 8: Change of instruction lengths between the original and the selected subset from WizardLM-70K dataset.